Starch Fractions as Examples for Nonrandomly Branched Macromolecules. 2. Behavior in the Semidilute Region

Gabriela Galinsky and Walther Burchard*

Institute of Macromolecular Chemistry, University of Freiburg, 79104 Freiburg, Germany

Received September 10, 1995; Revised Manuscript Received December 5, 1995[⊗]

ABSTRACT: In a former paper, the dimensional properties of degraded starch fractions of different molar masses were reported. The behavior was found to be dominated by the highly branched amylopectin. The same samples are now investigated in semidilute solution by static−dynamic light scattering. The deviating values of the overlap concentrations calculated by four definitions ($[\eta]$, R_g, R_h, and A_2) are discussed. The influence of polydispersity, excluded volume, and branching are checked. All starch fractions form one common master curve in the plot of the normalized osmotic modulus versus the reduced concentration (c/c^*). The data are described in terms of the third and fourth virial coefficients A_3 and A_4. At concentrations higher than 9%, low-angle excess scattering starts to govern the behavior in static light scattering, and simultaneously slow motion becomes noticeable in the time correlations function (TCF) that grows as the concentration is increased. The TCFs are described by stretched exponentials (KWW functions). Three modes are observed: a fast one *in*creasing with concentration and two other ones *de*creasing with concentration. The concentration dependencies of the first two motions are compared with the behavior of the cooperative and the reptation modes predicted by de Gennes for linear chains. The third (slow) motion is interpreted as being caused by associates.

Introduction

As pointed out in a previous paper,[1] most branched systems arise from random branching of multifunctional unimers or cross-linking (vulcanization) of linear chains. These systems are characterized by very broad size distributions and by the occurrence of gelation at a critical point of conversion of the functional groups.[2−4] Amylopectin and glycogen, on the other hand, are known as highly branched structures that belong to the class of hyperbranched macromolecules. These structures can never form a covalent gel.[2,5] The reason for this behavior results from constraints between the different reactive hydroxyl groups of the glucose unit at the C1, C4, and C6 positions. Due to the high specificity of enzymes, bonds can be formed only between C1 and C4 or C1 and C6.

This constraint of reactivity has a big influence on the width of the molar mass distribution and, thus, also on the dimensional properties.[5] The global properties (i.e., R_g, R_h, $[\eta]$, and A_2 as a function of M_w) of starch fractions in dilute solutions have been reported in part 1.[1] In this second part, we now deal with the behavior in semidilute solutions, which we expected to differ from that of linear chains.

This paper is divided into three parts: in the first, the molar mass dependence of the overlap concentration is considered. Second, we examine interactions among the branched macromolecules on the basis of their forward scattering behavior as a function of the concentration c, which is a measure of the inverse osmotic compressibility. Finally, the dynamics of the branched macromolecules is discussed. In addition, a rather extended outline of the theoretical background is given. We considered this part to be necessary since these theories have been developed for linear chains, and in applying them to branched materials, the background has to be carefully kept in mind.

Experimental Section

Starch Fractions.[1] Potato starch from Cerestar, Vilvorde, Belgium, was degraded in an alcoholic suspension at room temperature by adding different amounts of concentrated HCl. This is a procedure described by Fox and Robyt.[6] The starch fractions of different molar masses (between 30 000 and 10^8 g mol^{-1}) were the same as used in part 1, and their dimensional properties in 0.5 N NaOH were reported in our former paper.[1] In addition, four samples were prepared to obtain a comprehensive picture of the properties in the range of high molar masses (because of special interest in the angular dependence). All samples contain the large, highly branched amylopectin and up to 21% of the much smaller, linear amylose; but the dimensional properties in dilute solution are determined only by amylopectin.[1]

Static light scattering measurements were performed at 20°C with a fully computerized and electronically modified SOFICA photogoniometer (Baur, Instrumentenbau, Hausen, Germany) in the angular range from 30° to 140° in steps of 5°. An argon ion laser ($\lambda_0 = 488$ nm) and a helium/neon laser ($\lambda_0 = 632$ nm) were used as light sources. A refractive index increment of 0.142 was used for the measurements in 0.5 N NaOH.[7]

Dynamic light scattering measurements were made with an automized ALV goniometer and an ALV 5000 correlator/structurator in the multi-τ mode (from 30° to 150° in steps of 20°). Since the signal to noise ratio decreased for the more concentrated solutions, the pinhole was changed from 400 μm to 200 and 100 μm to omit this effect.

The solutions were filtered through Millipore filters (0.22 μm for the small M_w and up to 5 μm for high M_w and rather concentrated solutions). Only for really highly viscous, concentrated solutions was filtration no longer feasible. No heterodyne scattering was observed.

Theory

Overlap Concentration. A solution of concentration higher than a certain value c^*, at which point the overall concentration equals the segment concentration in one swollen coil, is called semidilute. De Gennes introduced the name "overlap concentration" for c^* since linear chains may be visualized as interpenetrating coils that eventually become entangled. At $c > c^*$ a drastic change in the properties is expected and also generally observed. Although the picture of chain overlap may be problematic with branched structures, the outer chains of the starch-type branched macromolecules still can penetrate each other in a manner similar to that of linear chains. For this reason, the term overlap concentration is used throughout this paper. The overlap

[⊗] Abstract published in *Advance ACS Abstracts,* February 1, 1996.

0024-9297/96/2229-1498$12.00/0

concentration is not only a boundary separating the dilute from the semidilute regimes it is also a key parameter in the theories of semidilute solutions. Unfortunately, c^* cannot be uniquely defined, and several definitions exist that can differ up to a factor 10. For flexible linear chains, the following conventions are accepted:[9]

$$c^*_{[\eta]} = 1/[\eta] \tag{1}$$

$$c^*_{R_g} = M/(N_A(4\pi/3)R_g^3) \tag{2}$$

$$c^*_{R_h} = M/(N_A(4\pi/3)\ R_h^3) \tag{3}$$

$$c^*_{A_2} = 1/A_2M_w \qquad (\textit{good solvent}) \tag{4}$$

The first is an equation for coils; for hard spheres the right-hand side has to be replaced by the expression 2.5/$[\eta]$. In the next two definitions, the dimension of the coils is described by equivalent spheres, and the last one results from thermodynamic interactions. The four relationships for the overlap concentration are mostly assumed to be proportional to each other. Apparently this is the case for linear chains, but, as will be shown later, these quantities show different molar mass dependencies for the present branched materials. Hence, depending on which definition for c^* is taken, different conclusions could be drawn.

Static. A description of behavior in the semidilute regime is not a trivial problem. The molecules are not isolated, and strong thermodynamic and hydrodynamic interactions start to dominate the properties. The well-established procedures, which enabled the interpretation of data in dilute solution, are not valid any longer. For instance, the angular dependence of the scattered light is now also a function of the concentration c, which is mathematically described by the structure factor $S(q,c)$:

$$R_\theta = KcS(q,c) \tag{5}$$

$$S(q,c) = S'(q,c)P(q)$$

Only for strongly interacting, hard spheres can $S(q,c)$ be described by theory, and it is factored into a particle scattering part, $P(q)$, and an *inter*particle scattering part, $S'(q,c)$. In all other cases this factorization is not strictly valid, but can still be used as a good approximation.[8,9] Fortunately, extrapolation to zero scattering angle θ ($q = 0$) is often possible, and now $S(q{=}0,c)$ is solely defined by thermodynamics.

(a) Virial Expansion. $Kc/R_{\theta=0}$ is given by the inverse osmotic compressibility that can be expanded in a virial series:

$$\frac{Kc}{R_{\theta=0}} = \left(\frac{1}{RT}\right)\left(\frac{\partial\pi}{\partial c}\right) = \frac{1}{M_w}(1 + 2A_2M_wc + 3A_3M_wc^2 + ...) \tag{6}$$

In the following, the inverse osmotic compressibility $(1/RT)(\partial\pi/\partial c)$ will be denoted as the osmotic modulus. The higher virial coefficients A_i are related to the second one:[9,10]

$$A_3M_wc^2 = g_A(A_2M_wc)^2 = g_AX^2 \tag{7}$$

$$A_4M_wc^3 = h_A(A_2M_wc)^3 = h_AX^3 \tag{8}$$

Table 1. The Structure Dependent Parameter g_A: Theoretical Values and Experimentally Determined by Fitting A_3[10]

architecture	g_A
stiff rod, infinitely thin	0.0[a,30]
flexible, linear chain	0.29 + 0.02
star molecule	
$f = 3$	0.35 + 0.01
$f = 12$	0.54 + 0.04
hard sphere	0.625[a,11]

[a] Theoretical values.

where the coefficients g_A and h_A are structure dependent. For hard spheres, they are all positive and known up to A_7.[11] For flexible chains, only A_3 is known (good solvent) to be $g_A = 0.277$,[12] in good agreement with the experimental finds of Kniewske and Kulicke[13] and of our own group.[10] For hard spheres a virial expansion up to A_3 fails if $A_2M_wc > 0.6$, and higher terms have to be taken into account; for flexible coils the corresponding limit is $(A_2M_wc) \geq 2.0$.

Several attempts have been made to calculate the higher virial coefficients for so-called soft spheres,[14,15] by applying the same cluster expansion that was used with success for hard spheres. McQuarrie[14] assumed a Gaussian density distribution of a soft sphere and calculated the various cluster contributions in three-dimensional space. Kosmas,[15] on the other hand, applied the RG theory and derived the cluster expansion in four-dimensional space, followed by an ϵ expansion to derive the results of three-dimensional space. Both the soft sphere and Kosmas treatment result in an alternating series of virial coefficients and are applicable only up to $A_2M_wc < 2$. Even in this region the derived relationships do not represent the linear chain, but rather structures that resemble branched materials. In contrast to hard spheres, the physical meaning of the higher virial coefficients for interpenetrating chains remains questionable.

Analytical expressions have also been derived for prolate and oblate ellipsoids[16] and for cylindrical structures of different axial ratios.

The parameter g_A was calculated and experimentally determined for different structures (see Table 1). The influence of polydispersity on g_A is not sufficiently well-known. Recent estimations by Stockmayer et al.[17] of polydispersity effects on A_2 and A_3 revealed deviations on the order of at most 20%, even for broad distributions, e.g., the LogNorm distribution.

We emphasize that the parameter h_A in eq 8 in particular is purely an empirical parameter and does not represent the effect of the fourth virial coefficient, but is probably a quantity that averages over the effect of even higher virial coefficients.

(b) Scaling Analysis. For the interpretation of semidilute solutions a new approach is necessary. Such an approach was proposed by de Cloiseaux[18] and de Gennes[19,20] for flexible linear chains. According to their model, linear chains, above the overlap concentration c^*, form a transient interpenetrating network. In such an entangled network, the measured values are no longer determined by the parameters of the single chain (e.g., radius of gyration R_g, molar mass M_w), but by a key parameter of the network, which is the correlation length ξ, and thus must be independent of the molar mass. Chains of the same structure but different length should develop the same behavior in the concentration dependence.

In the semidilute solution, the osmotic pressure is presumed to follow the asymptotic power law:[18]

$$\pi \sim \frac{c}{M}\left(\frac{c}{c^*}\right)^x \qquad c \gg c^* \tag{9}$$

The exponent x is fixed by the requirement that π must be independent of M for $c \gg c^*$ and by the relationship $c^* \sim M^{-z}$. For linear flexible chains in good solvents, where $\nu = 3/5$ in $R \sim M^\nu$, this means $c^* \sim M^{-4/5}$ (see eq 2), and together with the molar mass independence this leads to $x = 5/4$ (from $(3\nu - 1)^{-1}$). Thus,

$$\pi \sim c^{9/4} \tag{10}$$

$$\partial\pi/\partial c \sim c^{5/4}$$

However, chain stiffness, branching, and polydispersity have some influence, and the molecular mass dependence of the overlap concentration is not known in all cases. For comparison of different structures, it is convenient and common praxis to plot the normalized (reduced) osmotic modulus

$$\frac{M_w}{M_{app}} = \left(\frac{M_w}{RT}\right)\left(\frac{\partial\pi}{\partial c}\right) \tag{11}$$

versus the reduced concentration c/c^*. The osmotic modulus $(1/RT)(\partial\pi/\partial c)$ is a quantity that is measured by static light scattering at a concentration $c \neq 0$ and angle $\theta = 0$ (apparent molar mass M_{app}) and is only thermodynamically determined. Therefore, it is sensible to use the thermodynamic definition of c^* (eq 4), and to plot the osmotic modulus versus the scaling parameter $X = A_2 M_w c \equiv c/c^*$.

(c) Renormalization Group Theory. Ohta and Oono,[21] as well as Freed and his co-workers,[22] derived theoretical predictions for the whole region, from dilute to semidilute behavior, for flexible chains in a good solvent by using renormalization group (RG) methods. The exponent in the asymptotic power law is the same as predicted by scaling analysis ($x = (3\nu - 1)^{-1}$). But from this theory an exponent between $\nu = 0.588$[23] and $\nu = 0.592$[24] instead of Flory's 3/5 was found. These R_g exponents result in slightly larger values for $x = 1.31$ and $x = 1.29$, respectively, than that predicted by scaling arguments. For stars with a small number of arms ($f < 6$), the same exponent is expected from theory, but the many-arm systems are involved with theoretical problems,[22] which is reflected by poor predictions,[25] because of segment overcrowding.

From this theory it also follows that the osmotic modulus is a function of the reduced concentration c/c^*, and implies that $(c^*)^{-1} = A_2 M$. However, the scaling parameter $X_{th} = \langle A_2\rangle_w M_n c$ chosen in the theory is related to different averages from the experimental parameter $X_{ex} \equiv \langle A_2\rangle_{LS} M_w c$, where n, w, and LS denote number, weight, and LS averages, respectively.[26] Of course, for uniform samples the effect due to this difference does not exist. Polydispersity should shift the curve to lower X when plotting the osmotic modulus versus experimental values, but should not affect the asymptotic exponential behavior.[17] Similar conclusions were drawn by Trappe[27] with the Ohta−Oono expression for flexible chains.

Since computations on the basis of the RG theory are very complex, particularly for branched materials, Hager et al.[28] developed a semiempirical expression for a fit of experimental data:

$$\frac{M}{RT}\left(\frac{\partial\pi}{\partial c}\right) = 1 + 2X[1 + (q/p)2X]^p J(X) \tag{12}$$

with

$$J(X) = \left(\frac{1 + (q/p)X}{1 + (2q/p)X}\right)^p \left(1 + \frac{q}{2}\frac{X}{1 + (q/p)X}\right) \tag{13}$$

Expansion of this equation in powers of X identifies the parameter q as g_A, i.e., the ratio of the square of the second to the third virial coefficient, and for $X \gg 1$ the parameter p corresponds to the exponent x of the asymptotic power law $(M/RT)(\partial\pi/\partial c) \sim (c/c^*)^x$.

On the other hand, the osmotic modulus for hard spheres was calculated by Carnahan and Starling[29] (see Figure 4). Relationships are also available for rigid rodlike cylinders.[30]

Dynamics. The electric field time correlation function (TCF) $g_1(t)$ is related to the measured intensity TCF $g_2(t)$ by the Siegert relationship.[31] For a dilute solution it is common practice to determine the z-average relaxation time from a cumulant fit, i.e., by a polynomial in terms of delay time t for the logarithmic TCF. In semidilute solution more than one type of motion is present, and the cumulant procedure yields an obscured result that is a weighted function of the various relaxation processes. In such cases, the various parts of $g_1(t)$ can be approximated by a sum of stretched exponentials [Kohlrausch−Williams−Watts functions (KWW)].[32,33]

$$g_1(t) = a_1 \exp(t/b_1)^{\beta_1} + a_2 \exp(t/b_2)^{\beta_2} + \ldots \tag{14}$$

with $\sum a_i = 1$ and $0 < \beta \leq 1$.

The parameters a_i correspond to the weight of the various processes, and b_i and β_i characterize the mean relaxation time $\langle\tau_i\rangle$, which is given by

$$\langle\tau_i\rangle = \frac{b_i}{\beta_i}\Gamma\left(\frac{1}{\beta_i}\right) \tag{15}$$

where $\Gamma(x)$ is the Γ function. The parameter β is a measure for the width of the τ distribution, $\beta = 1$ corresponds to a single exponential and stands for a narrow distribution, and a smaller β means a broad distribution.

If $1/\tau$ is a linear function of q^2, the relaxation process is diffusive.[34] The diffusion coefficient of this motion is calculated from the mean relaxation time by eq 16, and the hydrodynamic radius is obtained from the diffusion coefficient by the Stokes−Einstein relation (eq 17):

$$D = 1/(\tau q^2) \tag{16}$$

$$R_h = \frac{k_B T}{6\pi\eta_0 D} \tag{17}$$

Equation 17 is applicable only to particles in dilute solution.

(a) Scaling Analysis. For the dynamic behavior of linear chains in semidilute solutions, de Gennes[19,35] predicted two types of motion: (i) a fast one, where the cooperative diffusion D_{coop} increases with the concentration and should be independent of the molar mass (it is connected to a hydrodynamic correlation length ξ by the Stokes−Einstein type of equation),[19] and (ii) a slower one, D_{rep}, that decreases with concentration and molar mass and originates from reptation, i.e., the motion of

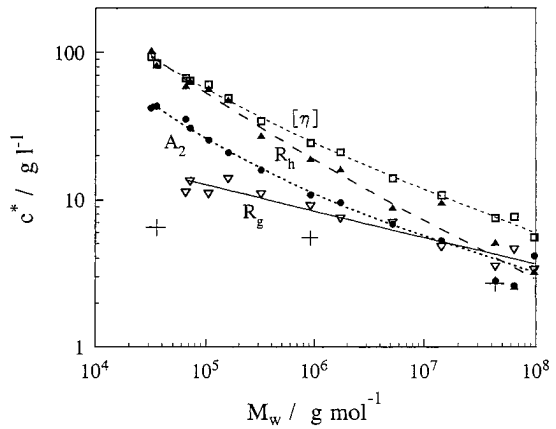

Figure 1. Overlap concentration c^* calculated from $[\eta]$ (□), R_g (▽), R_h (▲), and (●) A_2 (eqs 1−4) for the different molar masses. +, scaling parameters from Figure 9. The lines are to guide the eyes.

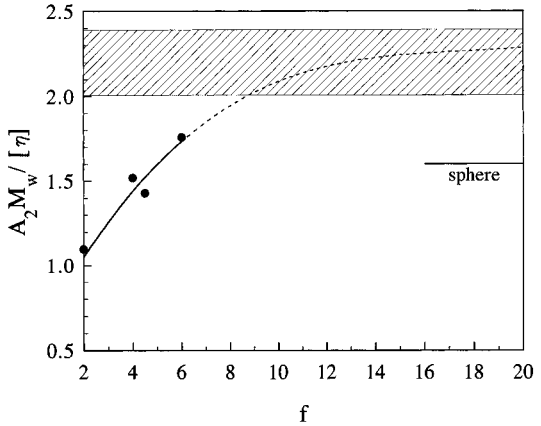

Figure 2. Theoretical values of the ratio $A_2M_w/[\eta]$ for stars[45] in depending on the number of arms (flexible ring: $f = 4.5$).[46] The shaded area denotes the experimental range of branched polymers (Figure 3a).

individual chains along their contour length through the entanglement network, which is described by a tube formed of the neighboring chains.[35,36] Linear chains in a good solvent should follow the relationships

$$D_{coop} = \frac{kT}{6\pi\eta_0\xi} \sim c^{3/4}M^0 \tag{18}$$

$$D_{rep} \sim \frac{R_{tube}^2}{\tau} \sim c^{-7/4}M^{-2} \tag{19}$$

For a linear chain in a θ solvent, de Gennes predicted a concentration dependence for D_{coop} with an exponent of 1.

Munch et al.[37,38] and Adam et al.[39] found exponents between 0.66 and 0.77 for semidilute solutions of PS and PDMS in good solvents. In the last time, tentative evaluation of the dynamic behavior was made by plotting D_{coop}/D_z (D_z diffusion coefficient at zero concentration) versus the scaling parameter $X = A_2M_wc$.[27,40] In contrast to expectation, no scaling behavior was observed for the various molar masses, and an exponent of 3/4 was not reached even for the largest molecules.

The slowly decaying reptation mode was first investigated by forced Rayleigh scattering[41] and then also found by dynamic light scattering by Chu and Nose.[42] Amis and Han[43] studied this mode for PS in THF by DLS. Only in a short concentration range did they find the exponent of −1.75. Extended investigations were made also by Brown.[44]

A good summary of the dynamic behavior in semidilute solution on the basis of scaling laws and a comparison of expected and experimental data are given in ref 20.

Results

Overlap Concentration. The molecular parameters in dilute solution, i.e., radius of gyration R_g, hydrodynamic radius R_h, second virial coefficient A_2, and intrinsic viscosity $[\eta]$, were determined and discussed previously.[1] With these data, the overlap concentrations c^*, as given by eqs 1−4 were calculated. Figure 1 shows the plot of c^* versus the molar mass. As expected, different curves were obtained for the four relationships. Two interesting observations can be made: (i) The curves determined from $[\eta]$ and A_2 have similar shapes but are shifted vertically by a factor. (ii) The curves calculated from R_g and R_h have quite different slopes (influence of the ρ parameter, see part 1), but for c^* of low molar masses, the curve from R_h merges with the curve from $[\eta]$.

The fact that c^* from $[\eta]$ differs from that from A_2 is not surprising, although for linear chains almost identity is found because the former is based on a hydrodynamic volume and the other is based on a thermodynamically defined volume. The ratio of these two experimental quantities ($A_2M_w/[\eta]$) is 2.2 ± 0.2. This value may be compared with those observed and calculated for other geometrical structures. For hard spheres one has $A_2M_w/[\eta] = 1.6$, for linear chains 1.10 was derived by the RG theory (experiment 1.04 ± 0.10), for star-branched molecules the values are 1.52 for $f = 4$ and 1.73 for $f = 6$,[45] and for flexible rings ($f \cong 4.5$) the value is 1.43.[46] These data are plotted in Figure 2. It appears likely that the star-branched macromolecules will approach an asymptotic value that would be near the experimental data for the branched molecules. The increase in the mentioned ratio from 1.1 for linear chains[47] to 2.2 or 2.14 (fractionated branched polycyanurates)[48] for the branched ones may result from the asymptotic coil penetration function Ψ^* that increases more strongly with branching than the Fox−Flory parameter Φ in the intrinsic viscosity (Figure 3). The decrease to 1.6 for the hard sphere is a little unexpected, but may result from the smooth and well-defined surface, which has a noncomparable effect on the hydrodynamics.

Isihara and Hayashida[49] calculated the ratio for prolate ellipsoids and reported an increase in this ratio with the axial ratio. However, by using the equations for cylinders, as given by Yamakawa,[50] one finds a continuous decrease, and a similar result is obtained when the Simha equation for viscosity[51] is used together with Isahara's expression for A_2. Isahara et al. probably made a trivial numerical error.

On the other hand, R_h and $[\eta]$ are both hydrodynamic quantities, but they are influenced differently by the hydrodynamics. Thus, the overlap concentration need not display the same molar mass dependence. Only in the limit of low molar masses do the two curves coincide. The various weighting of averages for R_h rather than for $[\eta]$ could be one reason, because a correction would result in higher c^* from R_h ($c^* \sim M_w\langle 1/R_h\rangle_z^3$) than from $[\eta]$ ($c^* \sim M_n/\langle R_g^3\rangle_n$). In Figure 2b the ratio $c^*_{R_h}/c^*_{[\eta]}$ is plotted. The theoretical curves were calculated by taking into consideration the polydispersity of the ABC

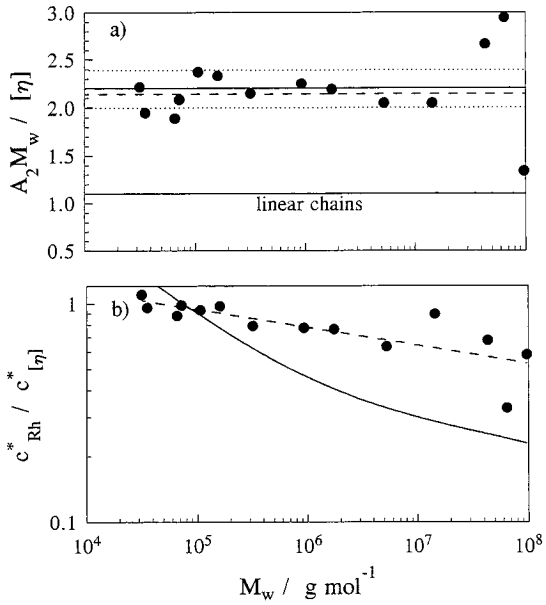

Figure 3. (a) Ratio $A_2M_w/[\eta]$ as a function of the molar mass of starch (●). The dotted lines denote the range of experimental errors, and the dashed line indicates fractionated branched polycyanurates.[48] (b) Ratio of the overlap concentrations from both hydrodynamic definitions. The solid line indicates theoretical curve when polydispersity is taken into account.

polycondensation model. The approximation

$$\frac{M_w}{M_n}\langle R_g^3\rangle_n\left\langle\frac{1}{R_h}\right\rangle_z^3 \simeq \frac{M_w}{M_n}\rho^3\left(\frac{M_n}{M_z}\right)^{3\nu_{R_g}} \qquad (20)$$

was made and the curve was calculated for $\nu_{R_g} = 0.39$ (see part 1). Expressions for M_n, M_w, M_z, and ρ were taken from the literature.[52] This theoretical curve decreases even more strongly with molar mass than the experimental values and indicates that the polydispersity is indeed the main reason for the stronger decay of $c^*_{R_h}$ in Figure 3b than of $c^*_{[\eta]}$.

Another factor to be considered is the influence of excluded volume. In their theories, Kurata and Yamakawa[53] derived different dependencies for the intrinsic viscosity $[\eta]$ and the friction coefficient Ξ (proportional to the hydrodynamic radius R_h) as a function of the expansion factor $\alpha = R_g/R_{g,\theta}$, where $R_{g,\theta}$ corresponds to the unperturbed dimension. This dependence can be described in general terms by $c^* \sim \alpha^{-x}$, where the exponent for $c^*_{[\eta]}$ is $x_{[\eta]} = 2-2.43$ in the region from freely drained to nondrained coils, but it is $x_{R_h} = 0-1.96$ for $c^*_{R_h}$. This would result in a stronger decrease in the overlap concentration with the molar mass for $c^*_{[\eta]}$ than for $c^*_{R_h}$. However, the opposite behavior was obtained. Hence, the theoretical molar mass dependence of $c^*_{R_h}/c^*_{[\eta]}$ should be slightly less than that shown in Figure 3b and, thus, comes closer to the experimental curve.

However, we have to emphasize that all of these conclusions are based on theories for *linear* chains, and conclusions on branched materials have to be considered with caution. No theories are available so far for branched structures. Certainly the branched molecules become more sphere-like, but the hydrodynamic properties cannot be directly compared with those of hard spheres since spheres have a smooth and well-defined surface, whereas the highly branched macromolecules will more resemble spheres with hairy chains on the surface. This hairy periphery very likely may cause a higher viscosity, which now will bring $c^*_{[\eta]}$ closer to that derived from R_h.

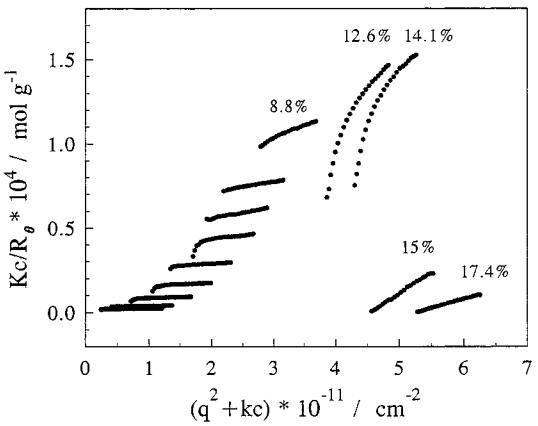

Figure 4. Zimm plot of sample LD11 (M_w = 920 000 g/mol) in the concentration range 0.7−18%.

Osmotic Modulus. In Figure 4 is given an example of a Zimm plot that covers the whole concentration region in our experiments. Three parts can be recognized: (i) In dilute solution, a low angular dependence is found and the concentration dependence seems to be linear. (ii) A transition to the semidilute region follows. The concentration dependence is no longer linear but develops a marked upturn. Furthermore, a strong angular dependence (so-called low-angle excess scattering) becomes noticeable, and the region gradually expands with c. (iii) In the last region this strong excess scattering has extended to high angles and governs the behavior. The concentration dependence shows a turnover and then decreases sharply. This turnover occurs for all samples at a concentration of 9 ± 1%. For the high molar masses, the excess scattering starts already at low concentration (3%) and the turnover region becomes broader, but the position of the maximum remains unchanged. The excess scattering is a sign for very large clusters or associates.[54,55] These grow very quickly in size as the concentration is increased.

For further evaluation, all scattering curves of various concentrations were extrapolated to $q = 0$, disregarding the excess scattering. The so-derived quantities are the inverse osmotic compressibilities, which for simplicity will be denoted as the osmotic modulus. Surprisingly, the points from all molar masses, in the range from 30 000 to 43 × 10^6 g/mol, form one common master curve (Figure 5). Such behavior is a sign of self-similar structures (the same branching density for all samples). An influence of increasing polydispersities with M_w could be expected from the RG theory. Evidently this influence is small. In this figure the sharp turnover for four of the samples is also plotted (but now the reduced concentration c/c^* is used). For the high molar masses, the modulus curve could be realized up to high X values.

The analysis of the master curve in terms of virial coefficients (eqs 6−8) is better done in a plot of the normalized forward scattering $R_{\theta=0}A_2/K$ versus $X = A_2M_wc$ (see Figure 6). A good fit is obtained with parameters $g_A = 0.18 \pm 0.03$ and $h_A = 0.03 \pm 0.01$.

$$\frac{R_{\theta=0}A_2}{K} = \frac{X}{1 + 2X + 3g_AX^2 + 4h_A4X^3} \qquad (21)$$

In the past only a g_A fit ($h_A = 0$) was made, and a structure dependence of g_A was found from experiments. Some of the g_A factors were derived by theories (see

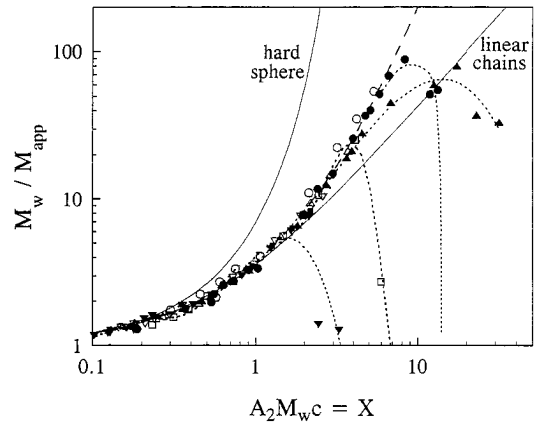

Figure 5. Osmotic modulus versus the scaling parameter $X = A_2M_wc$ for all samples (▼, $M_w = 35\,400$; □, $M_w = 105\,000$; ●, $M_w = 920\,000$; ▲, $M_w = 43 \times 10^6$ g/mol). The dashed line indicates the fitted curve with $g_A = 0.18 \pm 0.03$ and $h_A = 0.03 \pm 0.01$. The dotted lines indicate the onset of aggregation.

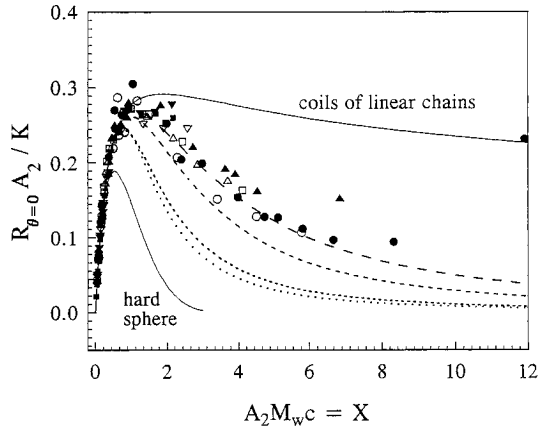

Figure 6. Normalized forward scattering, symbols as in Figure 5. The three additional curves correspond to crosslinked epoxies pre5, pre8, and pre10 measured by Trappe[27] (see Table 2).

Table 2. Structure Dependent Parameters g_A and h_A of the Virial Expansion, Experimentally Determined Including A_4 (eq 21), and Parameters of the Hager Fit[28] (eqs 12 and 13)[a]

	virial expansion		hager fit	
sample	g_A	h_A	$p = x$	$q = g_A$
starch	0.18 ± 0.03	0.03 ± 0.01	3.9	0.165
pre5 ($M_w =$ 172 000 g/mol)	0.183	0.067	9.4	0.190
pre8 ($M_w =$ 1.77×10^6 g/mol)	0.124	0.211	77	0.269
pre10 ($M_w =$ 13.6×10^6 g/mol)	~0	0.308	7600	0.292

[a] pre5 to pre10 are epoxy resins of increasing branching density and pregel samples.[27]

Table 1). One result was a decrease in g_A with growing stiffness. To describe the strong decrease in the curve at large X, i.e., after the maximum, it was necessary to include the fourth virial coefficient A_4 ($h_A \neq 0$). This was done first by Trappe[27] for anhydride-cured epoxies. She found a decrease in g_A and an increase in h_A with increasing extent of branching and molar mass of the pregel samples. The parameters found for amylopectin fit well into her series (see Table 2 and Figure 6). A decrease in g_A could be an indication of increasing stiffness with branching density and could be interpreted by a stretching out of the inner coil segments due to segment overcrowding. However, the apparent correlation between g_A and h_A indicates that these two factors have to be considered as mere fitting parameters.

A fit of the data was also attempted with the semiempirical equation by Hager et al.[28] (eqs 12 and 13), but the fits were successful only for $J(x) = 1$, which would not be fully consistent with the theoretical derivation. Increases in the exponents $p = x$ and the prefactors $q = g_A$ were found for starches and cured epoxies as a result of increasing branching density (see Table 2). The strongly increasing exponent could be expected since with increasing branching the macromolecules start to resemble hard spheres, which exhibit a divergence at $X \cong 3$ (close sphere packing).

Up to this point we have discussed only how the osmotic modulus curve can be fitted, which in its essence is an empirical treatment. A quantitative interpretation of these curves on the basis of a fundamental theory is not yet possible for the multiple-branched chains. Attempts to calculate the behavior were made for star-branched macromolecules on the basis of RG theory, but this treatment did not give fully satisfying results even for star-branched molecules with less than eight arms. The experimental curves appear shifted toward the hard sphere behavior more strongly than predicted. Ten years ago Witten et al.[56] gave a hint of a reasonable explanation, which is based on the Daoud–Cotton model[57] and the restricted segment interpenetration due to segment overcrowding near the center of the star. Thus, the central part of the star molecule already resembles a hard sphere. Taking this conception into account, the transition to hard sphere-like behavior becomes at least qualitatively understandable for the multiple-branched chains. However, this conception still does not explain the difference in behavior of the starch molecules compared to the randomly crosslinked epoxy chains. Of course, these two types of polymer differ in the type of molar mass distribution, which is much broader for the randomly crosslinked epoxies, and this might be one reason for the deviation. The other point is that the branching in starch is not fully random, but a correlated process, which may lead to a different capability for interpenetration of the outer chains. However, as long as no theory is available, we are not able to check these points quantitatively.

Dynamic Behavior. The intensity time correlation function (TCF) $g_2(t)$ of a dilute solution shows only one motion that is related to the translational diffusion of the branched particles. When going to higher concentrations, a second relaxation process becomes noticeable, which is in accord with the increasing excess scattering in the static light scattering experiments. Figure 7a shows an example of the angular dependence of $g_2(t)$ for a semidilute solution. The signal to baseline of the TCF's $g_2(t)$ was about 1.6 and was normalized to 2 for reasons of convenient comparison. As expected, the relaxation times of the two modes decrease with increasing scattering angle, and simultaneously the fraction of the slow mode also decreases. Another picture is obtained when considering the concentration dependence at a fixed angle (90°, Figure 7b). With increasing concentration the relaxation time of the fast mode decreases, but the relaxation time and the fraction of the slow mode increase. A more detailed, quantitative analysis revealed the slow motion to be composed of two modes. The fit by KWW functions made it clear that a good fit of the total TCF is possible only with three relaxation modes.

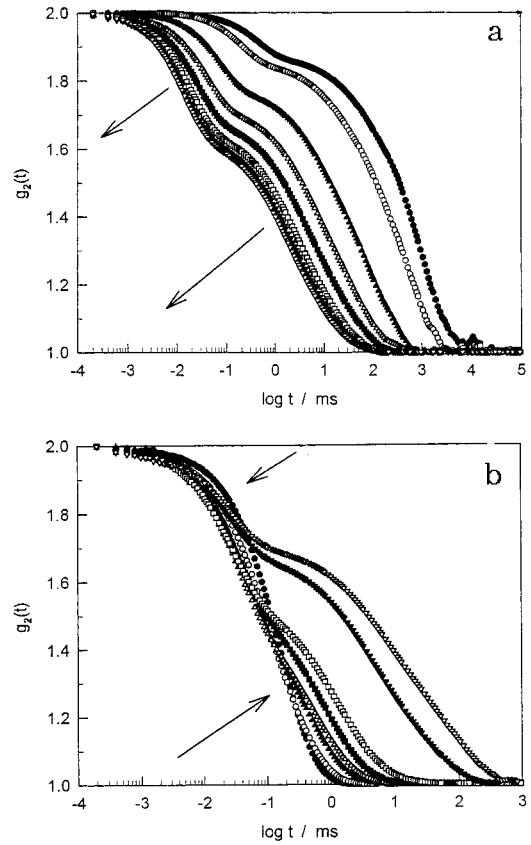

Figure 7. Normalized time correlation function $g_2(t)$ for sample LD11 (M_w = 920 000 g/mol): (a) angular dependence (●, 20°; ○, 30°; ▲, 50°; △, 70°; ■, 90°; □, 110°; ▼, 130°; ▽, 150°); (b) concentration dependence (●, 0.7%; ○, 2.5%; ▲, 5%; △, 6.2%; ■, 7.1%; □, 8.8%; ▼, 12.6%; ▽, 14.1%). The arrows indicate increasing scattering and increasing concentration, respectively.

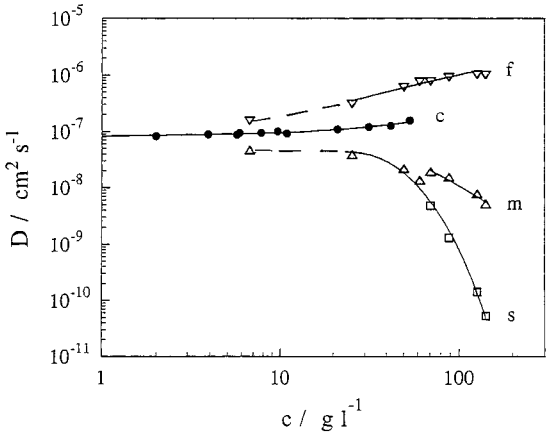

Figure 8. Concentration dependence of diffusion coefficients for sample LD11 (M_w = 920 000 g/mol): (f, ▽) fast motion, β = 1, angular independent; (m, △) medium motion, $\beta \approx 0.8$, in the three-motion fit angular independent; (s, □) slow motion, β decreasing, strong angular dependence; (c, ●) cumulant results. The f, m, and s modes were determined by KWW fits.

Three samples—a small (35 400 g/mol), an intermediate (920 000 g/mol), and a large molar mass (43×10^6 g/mol)—were investigated in detail. In all cases, the TCFs at high concentrations had to be described by a sum of three KWW functions. Only in the transition region from the dilute to the semidilute solution could the curves be fitted by two modes. Figure 8 shows the results for the example of the intermediate molar mass. The TCFs of the dilute solutions were evaluated by a 3-cumulant fit, and the semidilute solutions

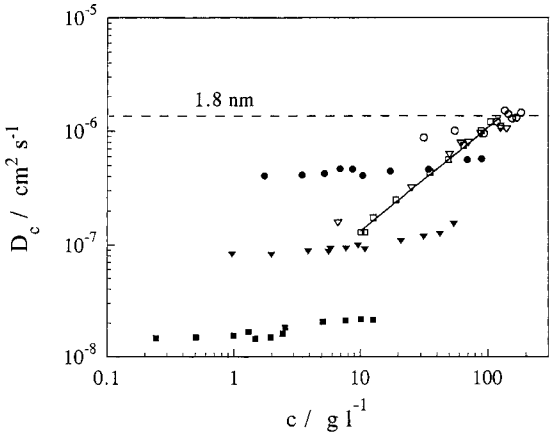

Figure 9. Cooperative diffusion coefficients (fast motion) for (○) LD8 (M_w = 34 500 g/mol), (▽) Ld11 (M_w = 920 000 g/mol), and (□) LD18 ($M_w = 43 \times 10^6$ g/mol). The slope of the curve is 0.9; filled symbols indicate the cumulant fit.

were described by the sum of two or three KWW functions.

The fast motion may be discussed first. This cooperative motion has no angular dependence, and the exponent in the KWW function was $\beta \cong 1$. This means a diffusive process of a monodisperse object, as expected for the cooperative diffusion. In Figure 9, the diffusion coefficients of the three samples are plotted versus the concentration. The three curves for the various molecular weights run into one common curve at large c. This behavior corresponds to the predictions by de Gennes for linear chains, according to which the properties become independent of the molar mass in the semidilute region and are only determined by the correlation length $\xi = kT/(6\pi\eta_0 D_{coop})$, which describes the mesh size of the transient network. The asymptotic slope in the present curve is 0.9; de Gennes predicted 0.75 for linear chains in a good solvent and 1 for a θ solvent. In the present case, however, the chains are branched, and for such structures no predictions are known to us. Furthermore, an upper limit seems to exist where no further increase in D_{coop} takes place. We are not fully clear whether this limit is caused by the limitation of the method of analysis or whether this limit is due to the system. The correlation length ξ in that limit corresponds to a distance of about 1.8 nm, which is approximately the length of maltotetraose.

The two other motions have very different concentration dependencies as the diffusion coefficients decrease. In the log−log plot, the second (intermediate) motions of the three samples seem to have the same slope. This resembles reptation modes for which de Gennes predicted a concentration dependence with an exponent of −1.75, but also a molar mass dependence (eq 19). Because of the limited molar mass range that was covered, the exact molar mass dependence was difficult to verify. We found an exponent of −0.7, which is considerably lower in value than the −2.0 predicted for linear reptating chains.

In Figure 10, the diffusion coefficients are normalized with respect to D_z, obtained at zero concentration. For the x coordinate, we looked for a scaling parameter. Master curves were obtained when dividing c by 6.5, 5.5, and 2.7 for the small, intermediate, and large molar masses, respectively. These scaling parameters should correspond to the overlap concentration $c^*_{R_h}$. Surprisingly, these parameters do not correspond to $c^*_{R_h}$, as expected, but apparently correspond much better to $c^*_{R_g}$

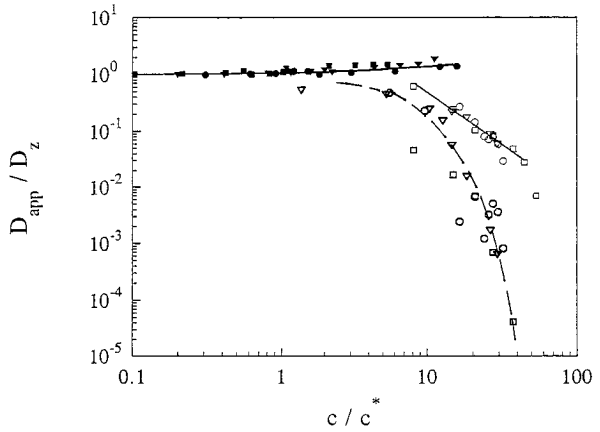

Figure 10. Diffusion coefficients of the medium and slow motions, normalized with respect to D_z at zero concentration as a function of c/c^*, the c^* values are given by the + symbols in Figure 1. Symbols as in Figure 8.

(see Figure 1). The physical meaning of these shift factors remained not clear to us.

The slope of the second motion is −1.85 and is also angular independent, and the β parameter of KWW functions is about 0.8; this could be an effect of polydispersity. For linear chains de Gennes predicted a slope of −1.75 as a result of chain reptation. The exponent −1.85 might be assigned to such a type of motion, but it is difficult to imagine the reptation of large branched macromolecules. In such cases, an exponential decrease rather than power law behavior should be observed, and in fact the points of measurements could likewise be fitted by a bent curve. Possibly, however, it is the low fraction of amylose whose motion is observed here.

The behavior of the third motion is clearer. It has a strong angular dependence and β decreases from 0.7 to 0.5 with increasing concentration. These are evidently the associates that are formed with increasing concentration. Again, it appears inconceivable that such extremely large clusters can move through the semidilute transient network, and in fact such slow motions completely disappear for covalently linked, permanent networks. Thus, the motion of the center of mass must result from the random forming and breaking of bonds, which indeed would result in an apparent motion of the clusters. We wish to emphasize that such slow motion was observed first by Amis et al.[58] with gelatin and confirmed by ter Meer with carrageenan.[59] In the mean time, a large number of other examples have been found, which in most cases were controversially interpreted.[20,44]

Summarizing Remarks

Three points have been treated in this paper. These are (i) the difference in the overlap concentration when using different molecular parameters, (ii) the concentration dependence of the osmotic modulus, and (iii) the dynamics of the semidilute solutions. The striking differences in the overlap concentration c^*, in particular the molar mass dependence, could be clarified as being mainly the result of polydispersity and different averaging, on the one hand, and of the differences between hydrodynamic and thermodynamic interactions. Thus, our paper may be considered as a first step to resolve the apparent differences in the definitions of c^*, which eventually may lead to algorithms for deriving the various concentrations c^* once one of the four overlap concentrations quoted in eqs 1−4 has been measured.

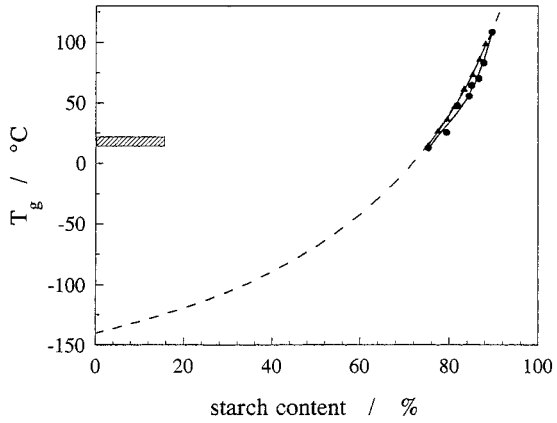

Figure 11. Glass transition temperature of amorphous amylopectin as a function of starch content (ref 62): ●, T_g by DSC; ▲, T_g calculated by using $T_{g,starch}$ = 500 K, dashed line, theoretical curve calculated by an equation given in ref 62. The shaded area denotes the range of measurement.

The osmotic modulus exhibits a concentration dependence between flexible interpenetrable chain molecules and impenetrable hard spheres, and this is evidently due to a hindered interpenetration of the outer chains. Each class of branched macromolecules showed self-similarity behavior, but differences between these classes still exist for reasons that remained to be clarified.

At concentrations higher than 9% all starch samples appear to cluster together, which is recognized by an onsetting sharp decrease in the osmotic modulus. Insight into this behavior could be obtained from dynamic light scattering. Pronounced slow motion commences at the same concentration where the osmotic modulus starts to decrease. This again confirms the clustering of chains. Three reasons for the appearance of slow motion are discussed in the literature. The rheological coupling that was brought forward by Brochard and de Gennes[60] can be excluded in this case because this would not be connected with the observed decrease in the osmotic modulus, with the low-angle scattering, and with the strong angular dependence of this mode.

Polymer physicists tend to interpret the clustering as an effect of glass formation.[61] Due to the thermal fluctuations, high segment accumulation may occur locally in the clusters, resulting in patches of glassy material, which, because of the frozen internal mobility, dissociate only slowly. We think that this interpretation can be excluded, because the effect occurs in our case in the range of 10−15%. Kalichevsky et al.[62] measured the concentration dependence of the T_g for starch and found a strong decrease with increasing water content, as is depicted in Figure 11. Extrapolations of this curve to 15% starch result in a glass temperature of about −120 °C, and this T_g appears too far away from the temperature of our measurements to exert a strong effect. Hence, the cluster formation is most likely a result of association due to intermolecular H-bonding, as is common for polysaccharides.[63]

The fast mode causes no problem since this corresponds to the common collective diffusion of the so-called pseudogel mode. To obtain a reasonable fit of the data, a further mode between the fast and slow motions had to be assumed. The exponent of concentration dependence of −1.85, together with the fact of no angular dependence of the diffusion coefficient, could give an indication of reptation, which appears in linear flexible chains in the semidilute regime. It is difficult to visualize a reptation with branched molecules. The

process of self-diffusion is certainly different since we observed a molar mass dependence with an exponent of −0.7, in contrast to that for linear chains of −2.0. On the other hand, Helmstedt[64] found a similar intermediate motion for branched polyethylene with a value of −1.9 for the exponent in the concentration dependence. Possibly the self-diffusion is not the result of the reptation, but rather an effect of the matrix reorganization.

Acknowledgment. We thank Dr. Jack F. Douglas, NIST, Gaithersburg, MD, for fruitful discussions. Robert Dolega, University of Freiburg, helped us with fitting programs for the interpretation of our data, which we gratefully acknowledge. The work was kindly supported by the Deutsche Forschungsgemeinschaft.

References and Notes

(1) Galinsky, G.; Burchard, W. *Macromolecules* **1995**, *28*, 2363.
(2) Flory, P. J. *Principles of Polymer Chemistry*; Cornell University Press: Ithaca, NY, 1953.
(3) Stockmayer, W. H. *J. Phys. Chem. II* **1943**, *11*, 45; **1944**, *12*, 125.
(4) Stauffer, D. *Introduction to Percolation Theory*; Tayler & Francis: London, Philadelphia, 1985.
(5) (a) Erlander, S.; French, D. *J. Polym. Sci* **1956**, *20*, 7. (b) Burchard, W. *Macromolecules* **1977**, *10*, 919.
(6) Fox, J. D.; Robyt, J. F. *Carbohydr. Res.* **1992**, *227*, 163.
(7) Huglin, M. L., Ed. *Light Scattering from Polymer Solutions*; Academic Press: London, New York, 1972.
(8) Guinier, A.; Fournet, G. *Small Angle Scattering of X-rays*; Jon Wiley & Sons: New York, 1955.
(9) Burchard, W. *Macromol. Chem., Macromol. Symp.* **1988**, *18*, 1.
(10) Burchard, W. *Macromol. Chem., Macromol. Symp.* **1990**, *39*, 179.
(11) Friedman, H. J. *A Course in Statistical Mechanics*; Prentice Hall: Englewood Cliffs, N.J. 1985; p 148.
(12) Douglas, J. F.; Freed, K. F. *Macromolecules* **1985**, *18*, 201.
(13) Kniewske, R.; Kulicke, W. M. *Macromol. Chem.* **1983**, *184*, 2173.
(14) McQuarrie, D. A. *Statistical Mechanics*; Harper & Row: New York, Evanston, San Francisco, London, 1976; p 252.
(15) Kosmas, M. K. *Macromolecules* **1989**, *22*, 720.
(16) Rigby, M. *Mol. Phys.* **1989**, *66*, 1261.
(17) Burchard, W.; Dolega, R.; Stockmayer, W. H. *Collect. Czech. Chem. Commun.* **1995**, *60*, 1653.
(18) des Cloizeaux, J. *J. Phys.* **1975**, *36*, 281.
(19) de Gennes, P.-G. *Scaling Concepts in Polymer Physics*; Cornell University Press: Ithaca, NY, 1979.
(20) Schäfer, D. W.; Han, C. C. In *Dynamic Light Scattering*; Pecora, R., Ed.; Plenum Press: New York, London, 1985.
(21) Ohta, T.; Oono, Y. *Phys. Lett.* **1983**, *79*, 339.
(22) Freed, K. F. *Renormalization Group Theory of Macromolecules*; Wiley & Sons: New York, 1987.
(23) Le Guillou, J. C.; Zinn-Justin, *J. Phys. Rev. Lett.* **1977**, *39*, 95.
(24) (a) Reference 22, p 147. (b) Vladimirov, A. A.; Kazakov, D. I.; Tarasov, D. V. *Sov. Phys. JETP* **1979**, *56*, 521.
(25) Douglas, J. F.; Roovers, J.; Freed, K. F. *Macromolecules* **1990**, *23*, 4168.
(26) Merkle, G.; Burchard, W.; Lutz, P.; Freed, K. F.; Gao, J. *Macromolecules* **1993**, *26*, 2736.
(27) Trappe, V. Ph.D. Thesis, University of Freiburg, Freiburg, Germany, 1994.
(28) Hager, B. L.; Berry, G. C.; Tsai, H. H. *J. Polym. Sci., Polym. Phys. Ed.* **1987**, *25*, 387.
(29) Carnahan, N. F.; Starling, K. E. *J. Chem. Phys.* **1969**, *51*, 635.
(30) Cotter, M. A.; Martire, D. C. *J. Chem. Phys.* **1970**, *52*, 1909.
(31) Siegert, A. J. F. *MIT Rad. Lab. Rep. No. 465,* **1943.**
(32) Kohlrausch, R. *Ann. Phys.* **1847**, *12*, 393.
(33) Lindsey, C. P.; Patterson, G. D. *J. Chem. Phys.* **1980**, *73* (7), 3348.
(34) Berne, B. J.; Pecora, R. *Dynamic Light Scattering*; Wiley & Sons: New York, 1976.
(35) de Gennes, P.-G. *Macromolecules* **1976**, *9*, 594.
(36) Leger, L.; Hervet, H.; Rondelez, F. *Macromolecules* **1981**, *14*, 1732.
(37) Munch, J. P.; Candau, S.; Herz, J.; Hild, G. *J. Phys. (Paris)* **1977**, *38*, 971.
(38) Munch, J. P.; Lemaréchal, P.; Candau, S.; Herz, J. *J. Phys. (Paris),* **1977**, *38*, 1499.
(39) Adam, M.; Delsanti, M.; Pouyet, G. *J. Phys. Lett. (Paris)* **1979**, *40*, L 435.
(40) Burchard, W.; Richtering, W. *Prog. Colloid Polym. Sci.* **1989**, *80*, 151.
(41) Hervet, H.; Leger, L.; Rondelez, F. *Phys. Rev. Lett.* **1979**, *42*, 1681.
(42) (a) Nose, T.; Chu, B. *Macromolecules* **1979**, *12*, 590. (b) Chu, B.; Nose, T. *Macromolecules* **1980**, *13*, 122.
(43) Amis, E. J.; Han, C. C. *Polymer* **1982**, *23*, 1403.
(44) Brown, W., Ed. *Dynamic Light Scattering*; Clarendon Press: Oxford, U.K., 1993.
(45) Douglas, J. F.; Freed, K. F. *Macromolecules* **1984**, *17*, 2344.
(46) Value of 4.37 in ref 45 has been corrected by J. F. Douglas to 1.43 (personal communication).
(47) Reference 22, p 238.
(48) Bauer, J.; Burchard, W. *Macromolecules* **1993**, *26*, 3103.
(49) Isihara, A.; Hayashida. T. *J. Phys. Soc. Jpn.* **1951**, *6*, 46.
(50) Yamakawa, H. *Modern Theory of Polymer Solution*; Harper & Row: New York, 1971.
(51) Simha, R. *J. Phys. Chem.* **1940**, *44*, 25. Mehl, J. W.; Oncley, J. L.; Simha, R. *Science* **1940**, *92*, 132.
(52) Reference 5a. Burchard, W. *Adv. Polym. Sci.* **1983**, *48*, 1.
(53) Kurata, M.; Yamakawa, H. *J. Chem. Phys.* **1958**, *29*, 311.
(54) Koberstein, J. T.; Picot, C.; Benoit, H. *Polymer* **1985**, *28*, 673.
(55) Gan, J. Y. S.; Francoise, J.; Guenet H.-M. *Macromolecules* **1986**, *19*, 173.
(56) Witten, T. A.; Pincus, P. A.; Cates, M. E. *Europhys. Lett.* **1986**, *2*, 137.
(57) Daoud, M.; Cotton, J. P. *J. Phys. (Paris)* **1982**, *43*, 531.
(58) Amis, E. J.; Janmey, P. A.; Ferry, J. D.; Hyuk, Y. *Polym. Bull.* **1981**, *6*, 13.
(59) ter Meer, H.-U. Ph.D. Thesis, University of Freiburg, Freiburg, Germany, 1985. Cited in Burchard W. *Macromol. Chem., Macromol. Symp.* **1990**, *39*, 179.
(60) Brochard, F.; de Gennes, P. G. *Macromolecules* **1977**, *10*, 1157.
(61) Koch, T.; Strobl, G.; Stühn, B. *Macromolecules* **1992**, *25*, 6255.
(62) Kalichevsky, M. T.; Jaroszkiewicz, E. M.; Ablett, S.; Blanshard, J. M. V.; Lillford P. J. *Carbohydr. Polym.* **1992**, *18*, 77.
(63) Jeffrey, G. A.; Sänger, W. *Hydrogen Bonding in Biological Structures*, Springer: Berlin, 1991; pp 214−219.
(64) Helmstedt, M. *Prog. Colloid Polym. Sci.* **1993**, *91*, 127.

MA9513527